Opto-mechanical Chiral Microrobot for Out-of-plane Rotation

Alaa M. Ali[a], Edison Gerena[b], Julio Andrés Iglesias Martínez[a], Gwenn Ulliac[a], Brahim Lemkalli[a], Abdenbi Mohand-Ousaid[a], Sinan Haliyo[b], Aude Bolopion[a], and Muamer Kadic[a]

[a]Université Marie et Louis Pasteur, Institut FEMTO-ST, CNRS, 25000 Besançon, France
[b]Sorbonne Université, CNRS, Institut des Systèmes Intelligents et de Robotique (UMR 7222 ISIR), Paris, France.

ABSTRACT

Optical tweezers use tightly focused laser beams to trap and manipulate microscopic particles by balancing scattering forces with a gradient force at the beam's focal point. This enables precise and contact-free particle control, making optical tweezers a powerful tool to activate microrobots (optobots) that give multiple degrees of freedom. However, realizing out-of-plane rotation, which is demanded for medical applications such as cell-manipulation and drilling, remains a challenge. Here, we present an optobot design leveraging chirality to achieve full-cycle out-of-plane rotation. This optobot has an elongated structure with dual optical handles and a chiral helix aligned on the long axis of the robot. The optical handles are used to be trapped by the optical tweezers beams to keep the long axis of the optobot and the helix perpendicular to the laser light propagation, while its chiral helical part generates out-of-plane rotation around its long axis under laser excitation due to broken axial parity. Finite element analysis was conducted to simulate the interaction of the chiral helix with the laser beam. The scattered beam distribution was visualized to see how it is altered by the chiral structure. The optical torque was also calculated to show that it is unidirectional following chirality. For experimental demonstration, the optobot was fabricated via two-photon lithography. The optical manipulation experiments using an optical tweezer system showed that the optobot demonstrates versatile actuation capabilities, achieving on-demand repetitive rotation, controlled-speed translation, and combined rotational-translational motion.

Keywords: Optical tweezers, Optical microrobots, Optomechanics, Chirality, Out-of-plane rotation

1. INTRODUCTION

The manipulation of microscopic objects has considerably advanced with the development of optical tweezers. Optical tweezers have highly focused laser beams to exert optical forces for precise control. Unlike conventional radiation pressure that creates scattering force pushing particles along the direction of light propagation, optical tweezers generate intensity gradients that allow stable trapping and precise manipulation of microobjects.[1] These tools have been widely used in nanotechnology, spectroscopy, quantum science, and particularly in biological applications, such as trapping viruses and bacteria,[2,3] as well as controlling cell transport and rotation.[4,5] However, direct laser exposure can damage cells, leading to the development of optically actuated microrobots (optobots) for safer and more precise manipulation. Optobots provide multi-degrees-of-freedom control by applying optical traps at specific points,[6] enabling functions like grasping,[7] cell transport,[8] and tele-operated microrobots with six-degree-of-freedom control.[9] While these systems have achieved in-plane motion, out-of-plane rotation remains a challenge despite its importance in medical applications such as microsurgeries, single-cell analysis, and microfluidic control.[10,11] Holographic optical tweezers can achieve out-of-plane rotation but are complex and expensive.[11] Planar time-multiplexing techniques offer a simpler alternative but are typically limited to in-plane motion.[12] Several approaches have been explored for out-of-plane rotation using planar optical tweezers, including curved structures that reorient under trap displacement,[11] jointed structures,[13,14] and paddle-wheel designs that rely on scattering forces.[15] However, these methods often suffer from limitations such as incomplete rotation cycles, instability, or low optical torque. Optical torque is typically normalized against

Further author information: (Send correspondence to A.A. and M.K.)
A.A.: E-mail: alaa.ali@femto-st.fr
M.K.: E-mail: muamer.kadic@univ-fcomte.fr

the maximum theoretically achievable value, which depends on factors like laser power, medium refractive index, and object geometry.[16,17] For example, a paddle-wheel design achieved only 9% of the maximum torque.[16] This paper introduces an optobot design utilizing chirality to achieve efficient out-of-plane rotation with high optical torque. Chiral structures can induce rotational motion under external forces, a principle widely used in fluid mechanics.[18] Recent studies have demonstrated that asymmetric optical structures can generate lateral forces and rotation.[19,20] Although previous designs utilized chirality induced in-plane rotation via polarization control,[16,21] our approach leverages chirality to give out-of-plane rotation. Our optobot has an arrow-like structure with a chiral tail. By applying an optical off-axis force to the chiral section, the design breaks axial symmetry and enables continuous out-of-plane rotation (Figure 1). This optobot has an elongated structure with dual optical handles and a chiral helix aligned on the long axis of the robot. The optical handles are used to be trapped by the optical tweezers beams to keep the long axis of the optobot and the helix perpendicular to the laser light propagation, while its chiral helical part generates out-of-plane rotation around its long axis under laser excitation due to broken axial parity. The idea of using chirality for out-of-plane rotation was introduced by our group,[22] and the design was experimentally tested, and it showed out-of-plane rotation (figure2) which gives potential to be used for various biomedical applications, including cell manipulation, rotation, and drilling. However, the aim of this study is to perform geometric optimizations to the helix by controlling the pitch distance in the helix, in order to achieve higher optical torque. Figure 1 shows the optimized optobot design with a pitch of $10\mu m$ that achieves a torque of 27%, which is higher than the previously proposed one of pitch $5\mu m$, which gave 17%.

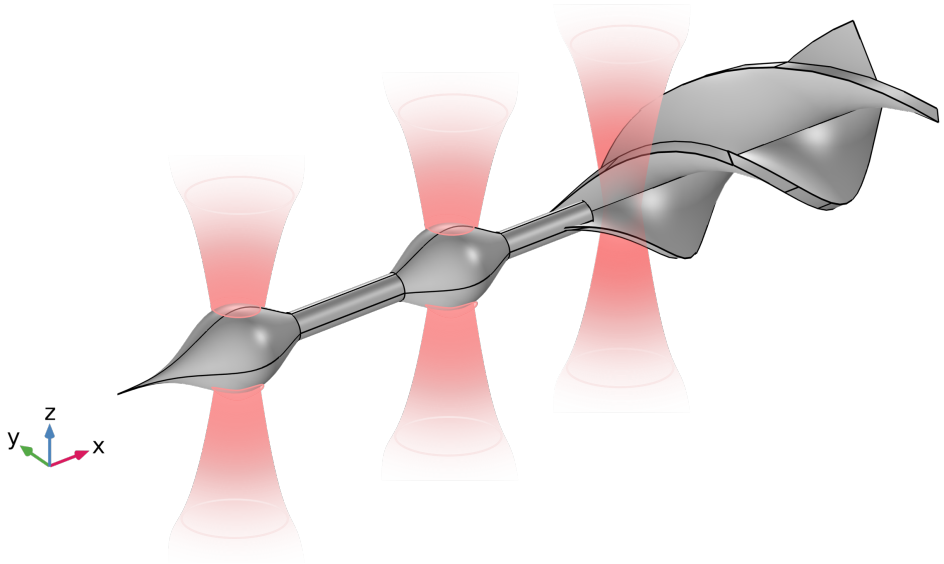

Figure 1. The optimized chiral optical microrobot to achieve out-of-plane rotation. Two optical handles are optically trapped by laser beams to keep the optobot horizontal and a third laser beam is directed to the helix of pitch $10\mu m$ to achieve out-of-plane rotation.

2. FINITE ELEMENT METHODS

The optomechanical properties of the optobot was anayzed by finite element method using COMSOL Multiphysics software. Firstly, using the radio frequency module, a Gaussian beam of linear polarization with a wavelength of 1070 nm was introduced in a water medium in the z-direction and directed to the chiral helix of the optobot with a refractive index of 1.5 to calculate the electromagnetic Maxwell Stress Tensor (MST) distribution on the helix. MST describes the transfer of electromagnetic momentum through space. It accounts for the mechanical stresses induced by electric and magnetic field components of the incident light. The tensor enables the force and torque calculations on objects due to electromagnetic fields. MST, denoted as $\mathbf{T}$, follows

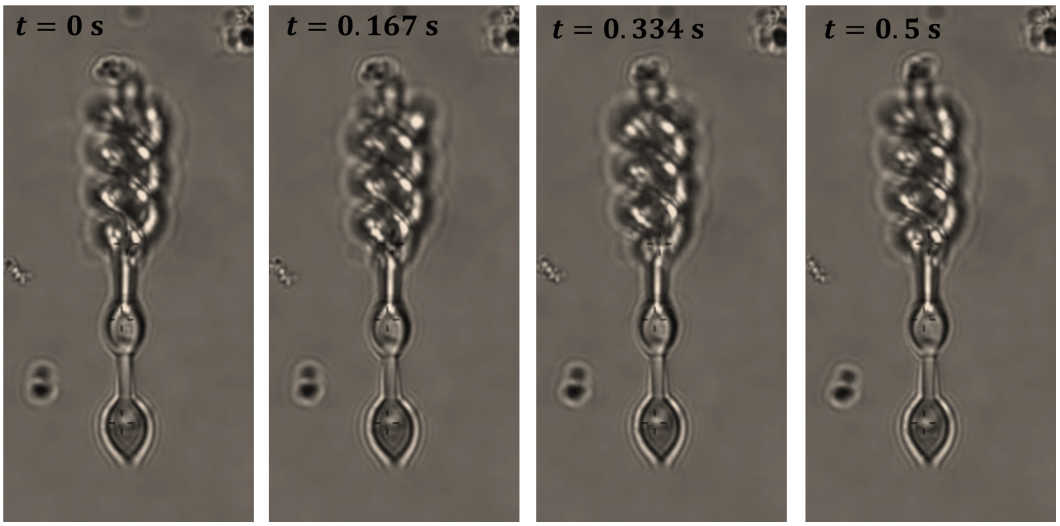

Figure 2. A label of "Video 1" which shows our previously proposed optobot giving out-of-plane rotation.[22] Screenshots for different orientations during its rotation. Here, the optobot returns to the same orientation after $0.5s$, and the average velocity of rotation is $0.4Hz$. The helix of this optobot has a pitch of $5\mu m$.

the expression:

$$T_{ij} = \varepsilon_0 \left(E_i E_j - \frac{1}{2}\delta_{ij}\mathbf{E}^2 \right) + \frac{1}{\mu_0} \left(B_i B_j - \frac{1}{2}\delta_{ij}\mathbf{B}^2 \right), \tag{1}$$

where ε_0 is the permittivity of free space, μ_0 is the permeability of free space, E_i and E_j are the components of the electric field vector $\mathbf{E}$, B_i and B_j are the components of the magnetic field vector $\mathbf{B}$, and δ_{ij} is the Kronecker delta, which is 1 if $i = j$ and 0 otherwise.

MST enables the computation of the optical force $\mathbf{F}$ on a particle via surface integration of the tensor$\mathbf{S}$, then the torque, $\boldsymbol{\tau}$, can be determined by the cross product between the force and the position vector $\mathbf{R}$.

$$\begin{aligned} \mathbf{F} &= \oint_S \mathbf{T} \cdot d\mathbf{S}, \\ \boldsymbol{\tau} &= \mathbf{R} \times \mathbf{F}, \end{aligned} \tag{2}$$

The MST gives a framework for analyzing how electromagnetic fields apply forces on objects. It establishes the relationship between the electric and magnetic fields giving insights into the resulting force distribution, providing precise analysis.

To standardize optical torque evaluation, it is typically expressed as as a normalized value, indicating the ratio of the calculated torque to the maximum theoretically optical torque to give a dimensionless measure that reflects the efficiency of the achieved torque in optical systems. The maximum theoretically achievable torque (τ_{max}) defines the highest output optical torque achievable by an optical system, influenced by optical power, refractive index, and object dimensions. It represents the upper limit of torque efficiency that is supposed to be reached under ideal conditions,[16,17] and it is calculated according to equation (3).

$$\tau_{max} = P \cdot n_m \cdot r/c, \tag{3}$$

where P is the laser power, n_m is the refractive index of the medium around the optobot, which is water of $n_m = 1.33$, r is the radius of the part of the helix interacting with the laser beam, and c is the light velocity.

3. DESIGN ENHANCEMENT BY GEOMETRY OPTIMIZATION

A helix is defined by several geometric parameters that determine its shape, size, and orientation. One of them is the pitch p: the axial distance between successive turns of the helix.

$$p = \frac{h}{N}, \tag{4}$$

where h is the total helix height and N is the number of turns. In this study, we worked the optimization of the pitch to give higher optical torque. A sweep was conducted for a range of pitches $4\mu m - 11\mu m$. For each pitch, the optical torque is calculated. As shown in figure 3, the optical torque increases by increasing the pitch distance. However, after $10\mu m$, we start to observe negative rotation. Therefore, the one that gives the most optimum results is the one with the pitch of $10\mu m$.

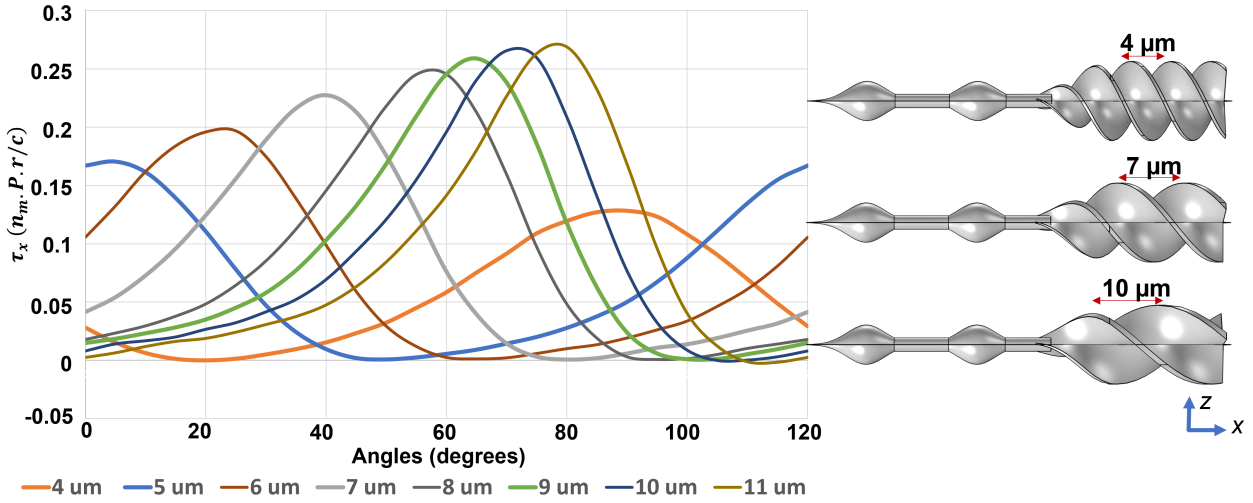

Figure 3. Calculations for the normalized optical torque of optobots with helices of different pitch distances. The normalized torque component τ_x is plotted against various angles spanning a full revolution of the OPTOBOT, ranging from 0 to 120°. This range represents the complete rotation due to the structure's C_3 rotational symmetry. Here, n_{m} denotes the refractive index of the surrounding medium (water), P is the laser power, r is the radius of the helical section interacting with the laser beam, and c represents the speed of light. The optobot with pitch $10\mu m$ showed the most optimum performance as the one with $11\mu m$ gives negative torque at angles 105°, and 110°.

4. OPTOMECHANICAL PROPERTIES OF THE OPTIMIZED OPTOBOT

In this section, the simulated optomechanical properties of the optimized optobt with pitch $10\mu m$ are shown. Numerical simulations indicate that the chiral tail breaks the axial parity; this can be observed through the asymmetric MST distribution over the surface of the helices shown in the insets of figure Figure 4 for different orientations of the helix during its rotation. Given the C3 symmetry of the helix, torque evaluations were conducted for angular positions from 0° to 120°, representing a full rotational period Figure 4. This figure shows the normalized optical torque, referenced against the theoretical maximum $\tau_{\max}$ (Equation 3), reaching 0.27 (27% of $\tau_{\max}$). Moreover, the resulting torque remains consistently positive, preventing reverse rotation. These findings demonstrate the efficiency of our optobot in enabling stable and controlled out-of-plane rotation.

5. CONCLUSION AND FUTURE WORK

In this article, chiral broken axial parity was leveraged to achieve a full-cycle out-of-plane rotation of a microrobot controlled by optical tweezers. We utilized three focal regions on the optobot: two optical traps to control its position and maintain horizontal stability, and one focal point on the chiral helix to generate rotation. Finite element simulations were conducted to investigate the optomechanical properties and determine the optimal pitch of the chiral helix to increase the optical torque. The results reveal satisfactory performance, with normalized optical torque exceeding previously reported values. Future work will focus on further optimizations of the chiral structure, including geometrical and topological optimizations, and the experimental testing of the optimized structures.

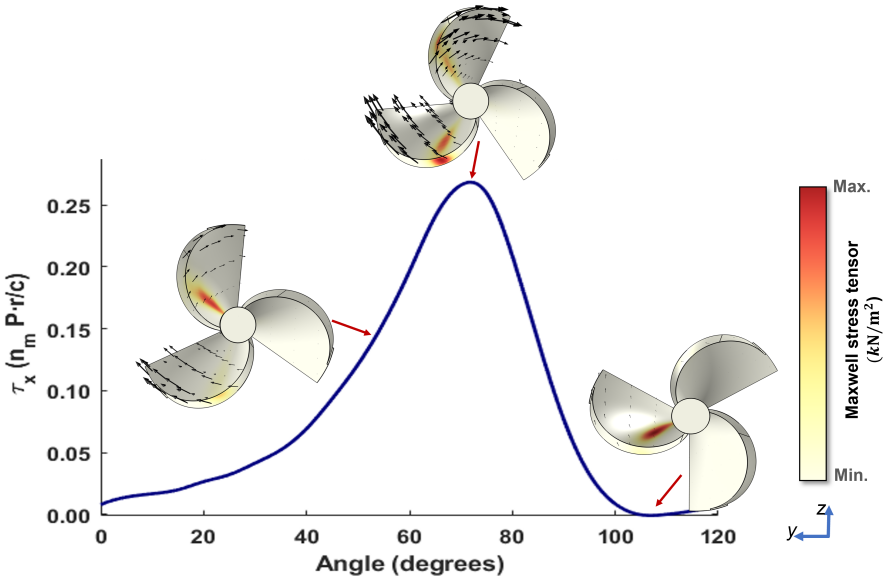

Figure 4. Simulation results for the chiral optobot. The normalized torque component τ_x is plotted against various angles spanning a full revolution of the OPTOBOT, ranging from 0 to 120°. This range represents the complete rotation due to the structure's C_3 rotational symmetry. Here, n_{m} denotes the refractive index of the surrounding medium (water), P is the laser power, r is the radius of the helical section interacting with the laser beam, and c represents the speed of light. The insets show the distribution of the Maxwell stress tensor at angles 55° representing medium torque, 75° which is the orientation giving the maximum torque, and angle 110° that has the minimum torque, the black arrows show the direction of motion where their length is proportional to the displacement.

ACKNOWLEDGMENTS

The authors acknowledge the support ANR OPTOBOTs project (ANR-21-CE33-0003), ANR PNanoBot (ANR-21-CE33-0015) and the Bourgogne Franche-Comté region through the project "platforme Robcell". The work was supported by the French RENATECH network and its FEMTO-ST technological facility MIMENTO. This work has been achieved in the frame of the EIPHI graduate school (contract "ANR-17-EURE-0002").

REFERENCES

[1] Yang, Y., Ren, Y., Chen, M., Arita, Y., and Rosales-Guzmán, C., "Optical trapping with structured light: a review," *Advanced Photonics* **3**(3), 034001 (2021).

[2] Ashkin, A., Schütze, K., Dziedzic, J., Euteneuer, U., and Schliwa, M., "Force generation of organelle transport measured in vivo by an infrared laser trap," *Nature* **348**, 346—348 (November 1990).

[3] Schimert, K. I. and Cheng, W., "A method for tethering single viral particles for virus-cell interaction studies with optical tweezers," *Proceedings of SPIE–the International Society for Optical Engineering* **10723**, 107233B (August 2018).

[4] Hu, S., Chen, S., Chen, S., Xu, G., and Sun, D., "Automated transportation of multiple cell types using a robot-aided cell manipulation system with holographic optical tweezers," *IEEE/ASME Transactions on Mechatronics* **22**(2), 804–814 (2017).

[5] Xie, M., Li, X., Wang, Y., and Sun, D., "Optical manipulation of cell rotation using a robust controller," in [*2015 IEEE 7th International Conference on Cybernetics and Intelligent Systems (CIS) and IEEE Conference on Robotics, Automation and Mechatronics (RAM)*], 36–41 (2015).

[6] Xu, B., Zhao, Y., Chen, X., Fu, R., Li, H., Xie, S., Liu, H., Li, Y., Zhang, S., and Li, B., "Power micromachines with light," *Laser & Photonics Reviews* , 2400791 (2024).

[7] Ta, Q. M. and Cheah, C. C., "Multi-agent control for stochastic optical manipulation systems," *IEEE/ASME Transactions on Mechatronics* **25**(4), 1971–1979 (2020).

[8] Dong, X., Hu, R., Wei, T., Chen, S., and Hu, S., "Indirect transportation of filamentous cells by using optically actuated microtools," in [*2019 IEEE/ASME International Conference on Advanced Intelligent Mechatronics (AIM)*], 1641–1645 (2019).

[9] Gerena, E., Legendre, F., Molawade, A., Vitry, Y., Régnier, S., and Haliyo, S., "Tele–robotic platform for dexterous optical single-cell manipulation," *Micromachines* **10**(10) (2019).

[10] Hu, S., Hu, R., Dong, X., Wei, T., Chen, S., and Sun, D., "Translational and rotational manipulation of filamentous cells using optically driven microrobots," *Opt. Express* **27**, 16475–16482 (Jun 2019).

[11] Zhang, D., Barbot, A., Lo, B., and Yang, G.-Z., "Distributed force control for microrobot manipulation via planar multi-spot optical tweezer," *Advanced Optical Materials* **8**(21), 2000543 (2020).

[12] Gerena, E., Régnier, S., and Haliyo, S., "High-bandwidth 3-d multitrap actuation technique for 6-dof real-time control of optical robots," *IEEE Robotics and Automation Letters* **4**(2), 647–654 (2019).

[13] Avci, E., Grammatikopoulou, M., and Yang, G.-Z., "Laser-printing and 3d optical-control of untethered microrobots," *Advanced Optical Materials* **5**(19), 1700031 (2017).

[14] Avci, E. and Yang, G.-Z., "Development of micromechanisms for handling of biomaterials under laser light," in [*2016 12th IEEE/ASME International Conference on Mechatronic and Embedded Systems and Applications (MESA)*], 1–5 (2016).

[15] Asavei, T., Nieminen, T., Loke, V., Stilgoe, A., Bowman, R., Preece, D., Padgett, M., Heckenberg, N., and Rubinsztein-Dunlop, H., "Optically trapped and driven paddle-wheel," *New Journal of Physics* **15**, 063016 (06 2013).

[16] Bianchi, S., Vizsnyiczai, G., Ferretti, S., Maggi, C., and Leonardo, R., "An optical reaction micro-turbine," *Nature Communications* **9** (10 2018).

[17] Rahimzadegan, A., Alaee, R., Fernandez-Corbaton, I., and Rockstuhl, C., "Fundamental limits of optical force and torque," *Phys. Rev. B* **95**, 035106 (Jan 2017).

[18] Collins, D. J. and Ligler, F. S., "Chiral microfluidics," *Lab on a Chip* **17**, 591–613 (2017).

[19] Arslan, D., Rahimzadegan, A., Fasold, S., Falkner, M., Zhou, W., Kroychuk, M., Rockstuhl, C., Pertsch, T., and Staude, I., "Toward perfect optical diffusers: dielectric huygens' metasurfaces with critical positional disorder," *Advanced Materials* **34**(5), 2105868 (2022).

[20] Nan, F., Rodríguez-Fortuño, F. J., Yan, S., Kingsley-Smith, J. J., Ng, J., Yao, B., Yan, Z., and Xu, X., "Creating tunable lateral optical forces through multipolar interplay in single nanowires," *Nature Communications* **14**(1), 6361 (2023).

[21] Rahimzadegan, A., Fruhnert, M., Alaee, R., Fernandez-Corbaton, I., and Rockstuhl, C., "Optical force and torque on dipolar dual chiral particles," *Phys. Rev. B* **94**, 125123 (Sep 2016).

[22] Ali, A. M., Gerena, E., Martínez, J. A. I., Ulliac, G., Lemkalli, B., Mohand-Ousaid, A., Haliyo, S., Bolopion, A., and Kadic, M., "Optical chiral microrobot for out-of-plane drilling motion," (2024).